

- ¹N. F. Ramsey and E. M. Purcell, *Phys. Rev.* **85**, 143 (1952).
- ²N. F. Ramsey, *Phys. Rev.* **91**, 303 (1953).
- ³E. A. G. Armour, *J. Chem. Phys.* **49**, 5445 (1968).
- ⁴E. Ishiguro, *Phys. Rev.* **111**, 203 (1958).
- ⁵T. P. Das and R. Bersohn, *Phys. Rev.* **115**, 897 (1959).
- ⁶M. J. Stephen, *Proc. Roy. Soc., Ser. A* **243**, 274 (1957).
- ⁷D. E. O'Reilly, *J. Chem. Phys.* **36**, 274 (1962).
- ⁸J. Schaefer and R. Yaris, *J. Chem. Phys.* **46**, 948 (1967).
- ⁹S. Ray, M. Karplus, and T. P. Das, unpublished.
- ¹⁰J. Goldstone, *Proc. Roy. Soc., Ser. A* **239**, 267 (1957).
- ¹¹C. M. Dutta, N. C. Dutta, and T. P. Das, *Phys. Rev. A* **1**, 561 (1970).
- ¹²D. R. Bates, K. Ledsham, and A. L. Stewart, *Phil. Trans. Roy. Soc. London, Ser. A* **246**, 215 (1953).
- ¹³D. R. Bates and R. H. G. Reid, in *Advances in Atomic and Molecular Physics*, edited by D. R. Bates (Academic, New York, 1968), Vol. IV, p. 13.
- ¹⁴D. R. Bates, U. Öpik, and G. Poots, *Proc. Phys. Soc., London, Sect. A* **66**, 113 (1953).
- ¹⁵K. Rüdénberg, *J. Chem. Phys.* **19**, 1459 (1951).
- ¹⁶M. Kotani, A. Amemiya, E. Ishiguro, and T. Kimura, *Tables of Molecular Integrals* (Maruzen Co. Ltd., Tokyo, 1955).
- ¹⁷H. P. Kelly, *Phys. Rev.* **131**, 684 (1963).
- ¹⁸H. P. Kelly, *Phys. Rev.* **173**, 142 (1968), and **180**, 55 (1969).
- ¹⁹N. C. Dutta, C. Matsubara, R. T. Pu, and T. P. Das, *Phys. Rev.* **177**, 33 (1968), and *Phys. Rev. Lett.* **21**, 1139 (1968).
- ²⁰T. F. Wimmatt, *Phys. Rev.* **91**, A476 (1953). Sign determined by I. Ozier, P. N. Yi, A. Khosha, and N. F. Ramsey, *Bull. Amer. Phys. Soc.* **12**, 132 (1967).
- ²¹S. D. Mahanti and T. P. Das, *Phys. Rev.* **170**, 426 (1968).
- ²²R. L. Matcha and W. B. Brown, *J. Chem. Phys.* **48**, 74 (1968).
- ²³J. Goodisman, *J. Chem. Phys.* **48**, 2981 (1968).

Formation and Structure of Electrostatic Collisionless Shocks*

D. W. Forslund and C. R. Shonk

Los Alamos Scientific Laboratory, University of California, Los Alamos, New Mexico 87544

(Received 4 November 1970)

A one-dimensional, two-species numerical-simulation code has been used to study the formation and structure of collisionless electrostatic shocks formed by two colliding plasmas and by a plasma striking a perfectly reflecting piston. Collisionless shocks are formed in hydrogen up to a maximum piston velocity of $M \equiv v_D/c_S \sim 3.5$. Shocks with velocities up to $M \sim 4$ have been produced which have a predominantly laminar structure accompanied by strong collisionless dissipation.

Theoretical models for electrostatic shocks in the absence of a magnetic field have been discussed by a number of authors.¹⁻⁵ Low-Mach-number [$M = v_D/c_S < 2$, where $c_S = (T_e/m_i)^{1/2}$] shocks have been experimentally produced by Alikhanov, Belon, and Sagdeev⁶ and Taylor, Baker, and Ikezi,⁷ and numerically simulated by Mason⁵ and Sakanaka, Chu, and Marshall.⁸ In this Letter we discuss formation of stable, high-Mach-number electrostatic shocks by means of the particle-in-cell simulation technique⁹ treating both the ions and electrons exactly with the mass ratio of hydrogen (1836). Since the electrons are treated exactly instead of isothermally, the critical Mach number of $M \sim 1.6$ does not apply. The shocks described here are well approximated by a rapid change from one equilibrium state to another with little or no fluctuations in the shock front (although perhaps having large fluctuations behind the front), and thus correspond most closely to the "laminar"¹⁻⁴ rather

than "turbulent"⁵ model.

Initial conditions.—The shocks discussed here are created in two ways. The first method consists of a plasma of ions and electrons moving to the right with Mach number M , as shown in Fig. 1(a), with the plasma initially ($T = 0$) just in contact with the right-hand, perfectly reflecting wall. The plasma is sustained at the left by continually injecting a Maxwellian plasma. The second method is similar but with the above plasma filling only the left half of the box and an equal-density plasma with Mach number of opposite sign occupying the right half. This configuration clearly should generate two shocks which differ only statistically. For $M < 1$ a shock will readily form on the basis of the ion-ion instability¹⁰ in one dimension. Shocks formed with $M > 1$ do so by means of the nonlinear process described below.

Theory of formation and structure.—In the two initial conditions used, the method of shock for-

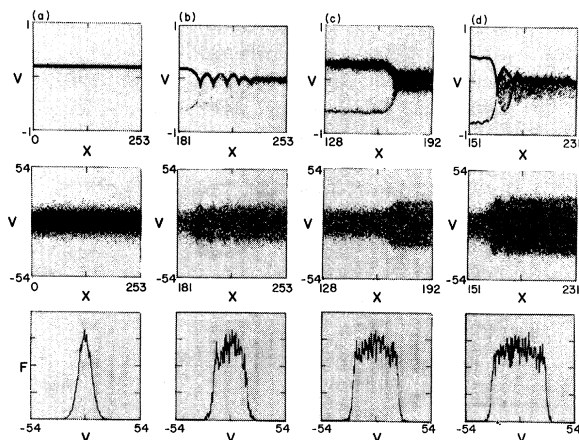


FIG. 1. Electrostatic shock ion and electron phase-space plots and electron distribution for $M=1.3$, $T_e/T_i=400$, at (a) $T=0$, (b) $T=298.2$; (c) $M=2$, $T_e/T_i=535.3$; and (d) $M=3$, $T_e/T_i=400$ at $T=1088.5$.

mation is essentially the same. An electrostatic sheath is formed on the edge of the plasma reflecting from the wall (as well as in each of the two colliding plasmas) which adiabatically traps the electrons, decelerates the incident ion beam, and accelerates the reflected ion beam. By assuming maximum-density trapping,¹¹ one can calculate the increase in density as a function of the potential jump as well as the increase in electron temperature. With the definitions $\psi = e\phi/kT_e$ where T_e is the initial electron temperature, n_1 the downstream density, and T_1 the downstream electron temperature, one obtains¹¹

$$n_1/n_0 = (2/\pi^{1/2})\psi^{1/2} + e^\psi \operatorname{erfc}(\psi^{1/2}), \quad (1)$$

$$\frac{T_1}{T_e} = \frac{n_0}{n_1} \left\{ \left(1 - \frac{2}{3}\psi\right)e^\psi \operatorname{erfc}(\psi^{1/2}) + \frac{2}{\pi^{1/2}}\psi^{1/2} \right\} + \frac{2}{3}\psi, \quad (2)$$

where $\operatorname{erfc}x$ is the complement of the error function. With the observed value of ψ , Eqs. (1) and (2) give good agreement with the density and temperature increases observed before the ions respond to form a shock. Since the density jump has a maximum around 2, Eq. (1) implies that there is a maximum potential of $\psi \sim 3$ that can exist in the interaction region. This in turn implies that there is a maximum deceleration of the ion beams and hence a critical Mach number. From Eq. (2) a maximum value of $\psi \sim 3$ implies a maximum value for $T_1/T_e \sim 3$ which, with conservation of energy for ions, gives an upper critical input Mach number $M_I \sim 3$. One expects an actual critical Mach number somewhat higher arising from the finite-amplitude ion waves of the electron-

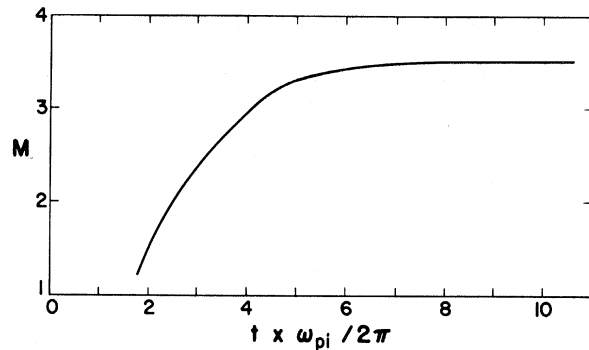


FIG. 2. Time for shock to form in ion plasma periods versus input Mach number.

ion instability. Figure 2 illustrates the dependence of formation time on input Mach number for the one-dimensional hydrogen plasma simulated here. The critical Mach number for this plasma appears to be about $M=3.5$. For Mach numbers somewhat above 3.5, and times somewhat longer than those shown in Fig. 2, the reflected and incident ion beams developed large-amplitude ion waves but did not interact with each other. For larger m_e/m_i , higher critical Mach numbers were obtained; but in the limit of infinitely light electrons, one would expect $M=3$ to remain a bound on the critical Mach number.

Once the shock has formed, Eqs. (1) and (2) also accurately describe the relationship between the observed jumps in density, potential, and electron temperature.

Numerical experiments.—A one-dimensional particle-in-cell computer program has been used to simulate the electrostatic interaction of electrons and ions in a manner similar to that of Morse and Nielson.⁹ Each of the electron and ion species is represented by from 25 000 to 80 000 simulation points which move in a linear grid of 1024 cells.

Figure 1 shows representative results for initial acoustic Mach numbers of 1.3 and 3 for $T_e/T_i=400$, and Mach number 2 for $T_e/T_i=9$. For homogeneous, counterstreaming beams with the above velocities, the equilibrium is stable in one dimension.¹⁰ In Fig. 1 length is measured in electron-Debye lengths λ_{De} , time in electron-plasma periods $\tau_{pe} = 2\pi/\omega_{pe}$, and velocities in units of $V_0 = \lambda_D/\tau_{pe}$. As a result of this scaling, the electron thermal velocity has the constant value $V_{th}^e \equiv (2kT/m)^{1/2} = 2\sqrt{2}\pi$. For clarity the electron distribution functions are normalized so the peak values are unity.

Columns (a) and (b) of Fig. 1 illustrate the case of input Mach number 1.3 for $T_e/T_i=400$ at time

Table I. Summary of electrostatic shock experiments.

$\frac{T_e}{T_i}$	M_I	M_S	$\frac{e\phi_S}{kT_e}$	$\frac{T_i}{T_e}$	$\frac{n_1}{n}$	$\frac{\lambda_{OSC}}{\lambda_{De}}$	$\frac{\lambda_S}{\lambda_{De}}$	$\frac{n_R}{n}$
400	0.5	1.5	$\sim .8$	1.2	1.4	6-7	~ 8	0
9	0.5	1.4-1.5	$\sim .6$	1.2	1.3	---	$\sim 6-7$	0
9	0.75	2.0	1.5	1.6	1.5	---	~ 8	$< .08$
400	1.3	2.6	3.3	2.4	2	7-8	~ 5	$< .01$
9	1.5	2.6	2.1	2.6	2	---	~ 8	$< .17$
9	2.0	3.2	4.2	3.7	2.4	---	~ 7	$< .15$
400	2.0	3.1	4.6	3.4	2.4	5-6	~ 5	$< .12$
400	3.0	4	8.2	5.2	3	~ 4	~ 5	$< .25$

0 and $298.2\tau_{pe}$. In Fig. 1 the first row is the ion phase space, the second row the electron phase space, and the third the electron distribution function. At time $T=0$ the electron distribution is averaged over the entire box; at later times it is averaged over a portion of the box behind the shock. The phase-space plots at later time are only portions of the whole box as indicated. Note the well-developed ion oscillations behind the shock and the small number of reflected ions for the case $M=1.3$. Because of the large trapping potential associated with the shock, the electrons have a marked increase in pressure behind the shock with secondary partial-trapping regions associated with the large-amplitude ion oscillations. The trapped-electron distribution is also characterized by its general flat-topped nature (bottom row, Fig. 1).

The observed parameters for the shocks studied are summarized in Table I. In the columns from left to right are, respectively, the temperature ratio T_e/T_i , the input Mach number, the resulting shock Mach number in units of the upstream ion acoustic speed, the potential jump across the shock in units of the upstream electron energy, the increase in electron temperature and density across the shock, the wavelength of the ion oscillations and thickness of the shock in upstream Debye lengths, and the fraction of ions reflected by the shock. It is important to note that the formula of Eq. (1) represents well the relationship between the increase in electron temperature, density, and potential across the shock suggesting that the electron trapping is nearly maximal. For the shocks with

initially very cold ions ($T_e/T_i=400$), the presence of reflected ions implies that the potential is very closely adjusted to the incoming ion energy ($e\phi \approx Mv_D^2/2$, or $e\phi/kT_e = M^2/2$). The electron trapping is particularly evident in motion pictures of phase space which have been made for the majority of the shocks listed in Table I. All of the shocks studied here have also maintained a very uniform velocity after the initial formation stages. In addition the shocks have been found to satisfy the Rankine-Hugoniot relations very closely.

In the Mach 2 case of Fig. 1(c) the ions are much hotter ($T_e/T_i=9$), which appears to completely damp the large-amplitude ion oscillations behind the shock. The ions do, however, appear to increase in temperature by about a factor of 3 in traversing the shock. In addition, the electron heating across the shock is larger than for the case of $T_e/T_i=400$ (see Table I), which is consistent with Eq. (2).

The Mach 3, $T_e/T_i=400$, case of Fig. 1(d) has been run to $T=1088.5\tau_{pe}$ ($\sim 25\tau_{pi}$) to illustrate the considerable ion trapping in the ion oscillations behind the shock (and consequent spatial damping) and the very steady behavior of the basic shock structure. The early-time character of this shock is very similar to that of Fig. 1(b).

On the basis of these experiments, one can reach a number of conclusions about the formation and structure of electrostatic shocks. First, the "laminar" type of shock has been shown to exist and to be stable for Mach numbers well above 1.5. Since turbulence is seen only behind the basic shock transition, what could be interpreted

as a "turbulent" shock has not been observed. Second, the existence of high-Mach-number electrostatic shocks appears to depend critically on the initial conditions used to form the shock. The electron trapping that occurs due to the interpenetration of the equal-density plasmas results in the reduction of the relative Mach number to the point where the electrostatic ion-ion instability¹⁰ can result in shock formation. This electron trapping does not occur in the homogeneous counterstreaming ion-beam problem¹² which leads to lower critical Mach numbers for strong ion-beam interaction.^{12,13} Third, this dependence on initial conditions suggests that with appropriate initial conditions, one could obtain even higher Mach number stable shocks than those found here. Whether these initial conditions could be realized in any laboratory plasma is an open question. This work is in substantial disagreement¹⁴ with the early work of Colgate and Hartman¹⁵ who, with nearly identical initial conditions, obtained electrostatic shocks with input Mach numbers >50 .

It should be noted that there is much similarity between these experiments and the particle observations in the Earth's bow shock reported by Montgomery, Asbridge, and Bame.¹⁶ The similar appearance of a flat-topped electron distribution behind, along with reflected ions in front, suggests that an electrostatic subshock may be

present in the Earth's bow shock.

*Work performed under the auspices of the U. S. Atomic Energy Commission and the Defense Atomic Support Agency.

¹S. S. Moiseev and R. Z. Sagdeev, *J. Nucl. Energy, Part C* **5**, 43 (1963).

²D. Montgomery and G. Joyce, *J. Plasma Phys.* **3**, 1 (1969).

³N. Yajima, T. Taniuti, and A. Outi, *J. Phys. Soc. Jap.* **21**, 757 (1966).

⁴R. J. Mason, *Phys. Fluids* **13**, 1042 (1970), and *Bull. Amer. Phys. Soc.* **14**, 1043, 1076 (1969).

⁵D. A. Tidman, *Phys. Fluids* **10**, 547 (1967).

⁶S. G. Alkhanov, V. G. Belan, and R. Z. Sagdeev, *Zh. Eksper. Teor. Fiz., Pis'ma Red.* **7**, 318 (1968) [*JETP Lett.* **7**, 405 (1968)].

⁷R. J. Taylor, D. R. Baker, and H. Ikezi, *Phys. Rev. Lett.* **24**, 206 (1970).

⁸P. H. Sakanaka, C. K. Chu, and T. C. Marshall, to be published.

⁹R. L. Morse and C. W. Nielson, *Phys. Fluids* **12**, 2418 (1969).

¹⁰T. E. Stringer, *J. Nucl. Energy, Part C* **6**, 267 (1964).

¹¹R. L. Morse, *Phys. Fluids* **8**, 308 (1965).

¹²D. W. Forslund and C. R. Shonk, *Phys. Rev. Lett.* **25**, 281 (1970).

¹³C. F. McKee, *Phys. Rev. Lett.* **24**, 990 (1970).

¹⁴J. M. Dawson, K. Papadopoulos, and R. Shanny, *Phys. Fluids* **13**, 1650 (1970).

¹⁵S. A. Colgate and C. W. Hartman, *Phys. Fluids* **10**, 1288 (1967).

¹⁶M. D. Montgomery, J. R. Asbridge, and S. J. Bame, *J. Geophys. Res.* **75**, 1217 (1970).

General Scheme of Studying Trapped Particles in Fusion Devices†

Chuan Sheng Liu* and Alfred Y. Wong

Department of Physics, University of California, Los Angeles, California 90024

(Received 7 October 1970)

A general scheme of detecting magnetically trapped particles in fusion devices through the observation of echo phenomena is proposed. The conditions for temporal echoes due to the trapped particles are derived and a physical explanation of trapped particle echoes is given.

We wish to propose a general scheme of demonstrating the existence of trapped particles between magnetic mirrors and investigating the lifetime, the orbit, and diffusion rate of such particles. Magnetically trapped particles have recently been shown to be important to the stability¹ and transport² of plasmas in toroidal systems. In this paper, we investigate echoes associated with these magnetically trapped particles and their possible experimental detection in the mir-

ror as well as toroidal systems such as multipoles and Tokamaks.

Our proposed scheme is stimulated by the recent observation of echoes due to ions trapped in electrostatic wells.³ The echoes which exhibit themselves as recurring radiation pulses at accurate intervals are contributed solely by trapped particles. Because phase information is involved these echoes are sensitive to diffusion, collisions, and plasma fluctuations. We shall present

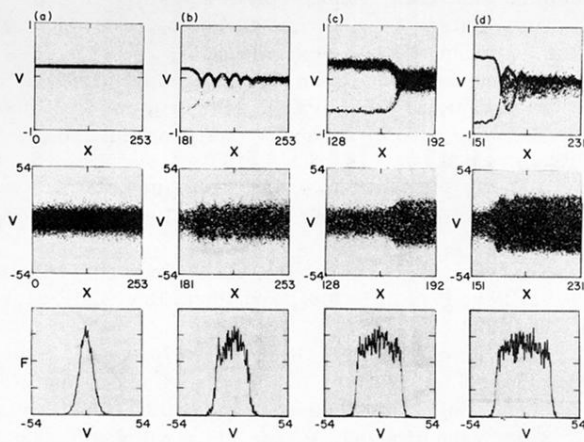


FIG. 1. Electrostatic shock ion and electron phase-space plots and electron distribution for $M=1.3$, $T_e/T_i=400$, at (a) $T=0$, (b) $T=298.2$; (c) $M=2$, $T_e/T_i=535.3$; and (d) $M=3$, $T_e/T_i=400$ at $T=1088.5$.